



HHS Public Access

Author manuscript

Cancer Discov. Author manuscript; available in PMC 2018 June 01.

Published in final edited form as:

Cancer Discov. 2017 June ; 7(6): 575–585. doi:10.1158/2159-8290.CD-16-1431.

An acquired HER2 T798I gatekeeper mutation induces resistance to neratinib in a patient with HER2 mutant-driven breast cancer

Ariella B. Hanker^{1,2}, Monica Red Brewer¹, Jonathan H. Sheehan^{3,4}, James P. Koch¹, Gregory R. Sliwoski⁵, Rebecca Nagy⁶, Richard Lanman⁶, Michael F. Berger⁷, David M. Hyman⁸, David B. Solit⁸, Jie He⁹, Vincent Miller⁹, Richard E. Cutler Jr.¹⁰, Alshad S. Lalani¹⁰, Darren Cross¹¹, Christine M. Lovly^{1,12}, Jens Meiler^{4,5}, and Carlos L. Arteaga^{1,2,12}

¹Department of Medicine, Vanderbilt University Medical Center, Nashville, TN, USA

²Breast Cancer Research Program, Vanderbilt-Ingram Cancer Center, Vanderbilt University Medical Center, Nashville, TN, USA

³Department of Biochemistry, Vanderbilt University, Nashville, TN, USA

⁴Vanderbilt Center for Structural Biology, Vanderbilt University, Nashville, TN, USA

⁵Department of Chemistry, Vanderbilt University, Nashville, TN, USA

⁶Guardant Health, Redwood City, CA, USA

⁷Department of Pathology, Memorial Sloan Kettering Cancer Center, New York, NY, USA

⁸Department of Medicine, Memorial Sloan Kettering Cancer Center, New York, NY, USA

⁹Foundation Medicine, Cambridge, MA, USA

¹⁰Puma Biotechnology, Inc., Los Angeles, CA, USA

¹¹AstraZeneca Pharmaceuticals, Cambridge, UK

¹²Department of Cancer Biology, Vanderbilt University Medical Center, Nashville, TN, USA

Corresponding Author: Carlos L. Arteaga, MD, Division of Oncology, Vanderbilt University Medical Center, 2220 Pierce Avenue, 777 PRB, Nashville, TN 37232-6307, Tel: 615-936-0975, Fax: 615-343-7602, carlos.arteaga@vanderbilt.edu.

Disclosure of potential conflicts of interest: R.N. and R.L. are employees of Guardant Health. J.H. and V.M. are employees of Foundation Medicine. R.E.C. and A.S.L. are employees of Puma Biotechnology. D.C. is an employee of AstraZeneca. Other authors declare no conflicts of interest.

Authors' Contributions

Conception and design: A.B. Hanker, M. Red Brewer, J.H. Sheehan, G. Sliwoski, J. Meiler, C.L. Arteaga

Development of methodology: A.B. Hanker, M. Red Brewer, J.H. Sheehan, G. Sliwoski, J. Meiler, C.L. Arteaga

Acquisition of data: A.B. Hanker, M. Red Brewer, J.H. Sheehan, J.P. Koch, G. Sliwoski, M.F. Berger

Analysis and interpretation of data: A.B. Hanker, M. Red Brewer, J.H. Sheehan, J.P. Koch, G. Sliwoski, R. Lanman, R. Nagy, M.F. Berger, D.M. Hyman, J. He, V. Miller, J. Meiler, C.L. Arteaga

Acquisition of clinical samples and/or collection/interrogation of patient data: R. Lanman, R. Nagy, M. Berger, D.M. Hyman, D.B. Solit, J. He, V. Miller, R.E. Cutler, Jr., A.S. Lalani, C.L. Arteaga

Writing, review, and/or revision of manuscript: A.B. Hanker, M. Red Brewer, J.H. Sheehan, G. Sliwoski, R. Lanman, D.M. Hyman, C.M. Lovly, J. Meiler, C.L. Arteaga

Provided reagents: D. Cross and C.M. Lovly

Participated in discussions: D.M. Hyman, R.E. Cutler, Jr., A.S. Lalani, D. Cross, C.M. Lovly

Study supervision: J. Meiler and C.L. Arteaga

Abstract

We report a HER2^{T798I} gatekeeper mutation in a patient with HER2^{L869R}-mutant breast cancer with acquired resistance to neratinib. Laboratory studies suggested that HER2^{L869R} is a neratinib-sensitive, gain-of-function mutation that upon dimerization with mutant HER3^{E928G}, also present in the breast cancer, amplifies HER2 signaling. The patient was treated with neratinib and exhibited a sustained partial response. Upon clinical progression, HER2^{T798I} was detected in plasma tumor cell-free DNA. Structural modeling of this acquired mutation suggested that the increased bulk of isoleucine in HER2^{T798I} reduces neratinib binding. Neratinib blocked HER2-mediated signaling and growth in cells expressing HER2^{L869R} but not HER2^{L869R/T798I}. In contrast, afatinib and the osimertinib metabolite AZ5104 strongly suppressed HER2^{L869R/T798I}-induced signaling and cell growth. Acquisition of HER2^{T798I} upon development of resistance to neratinib in a breast cancer with an initial activating HER2 mutation suggests HER2^{L869R} is a driver mutation. HER2^{T798I}-mediated neratinib resistance may be overcome by other irreversible HER2 inhibitors like afatinib.

Keywords

HER2; neratinib; gatekeeper mutation; breast cancer; precision medicine

Introduction

DNA sequencing efforts have revealed that *ERBB2*, the gene encoding the HER2 receptor tyrosine kinase (RTK), is mutated a wide variety of cancer types, including 2–3% of primary breast cancers (1–3), with a higher incidence in lobular breast cancers (4). More than 70% of HER2 mutations in breast cancer are found in the absence of *HER2* (*ERBB2*) gene amplification (2). Some of the common HER2 mutations promote HER2 kinase activity and transform breast epithelial cells and other cell types (5–9). Given that irreversible EGFR/HER2 tyrosine kinase inhibitors (TKIs) such as neratinib and afatinib have shown preclinical activity against several HER2 mutants (5,7–9), clinical trials with neratinib (SUMMIT trial; NCT01953926) and afatinib (NCI-MATCH; NCT02465060) focused in patients with HER2-mutant cancers are in progress. However, sustained clinical activity of ATP mimetics in patients with advanced cancer has generally been limited by the acquisition of drug resistance. Mutation of the “gatekeeper” residue within the kinase’s ATP-binding pocket, such as ABL^{T315I}, KIT^{T670I}, and EGFR^{T790M}, is a common mechanism of acquired resistance. Here, we report for the first time a case of a HER2 gatekeeper mutation in a patient with non-amplified HER2-mutant breast cancer with acquired resistance to neratinib.

Results

HER2 L869R exhibits a gain-of-function phenotype that is blocked by neratinib

Targeted capture next-generation sequencing (NGS) (10) of DNA from a skin metastasis in a 54 year-old female with ER/PR+, HER2 non-amplified lobular breast carcinoma identified an *ERBB2*^{L869R} (HER2^{L869R}) somatic mutation (Supplementary Table S1). Prior therapies included chemotherapy, tamoxifen, aromatase inhibitors, everolimus and trastuzumab. The tumor also harbored a truncation mutation in *CDH1*, *ERBB3*^{E928G} and amplification of

CCND1 and *FGF3/4/19*. Interrogation of cBioPortal (n>21,000), Project GENIE (n>18,000), COSMIC (n>50,000), Foundation Medicine (n>40,000), and Guardant Health (n>17,000) databases found 16 additional cancers harboring *ERBB2*^{L869R} and one L869Q mutation, including 12 breast cancers (Supplementary Table S2). Additionally, a recent study reported 4 instances of *ERBB2*^{L869R} among 413 invasive lobular breast cancers (4).

The L869R mutation is located within the activation loop of the HER2 kinase domain. Sequence alignment of the HER2, EGFR, and BRAF kinase domains showed that HER2^{L869R} is homologous to BRAF^{V600E}, a gain-of-function mutation found in >50% of melanomas (11), and EGFR^{L861R/Q}, an activating mutation in non-small cell lung cancer (NSCLC; Fig. 1A) (12). We performed structural modeling of the L869R mutation using Rosetta (13) and examined the residue pair energies involving L869. The mutation resulted in the addition of a strong attractive interaction between R869 and D769 (Fig. 1B,C). This interaction potentially stabilizes the active conformation of the C helix. We also predict that mutating L869 to a polar residue (Arg) disrupts the autoinhibitory contacts between the C helix and the activation loop helix, resulting in destabilization of the inactive conformation of the kinase, similar to EGFR^{L858R} (14).

Based on these structural data, we hypothesized that HER2^{L869R} would display increased signaling and transforming capacity. To test this, we stably transduced MCF10A breast epithelial cells with lentiviral vectors encoding HER2 wild-type (WT) or HER2^{L869R}. Cells expressing HER2^{L869R} exhibited increased phosphorylation of AKT, ERK, and S6, which were blocked by neratinib (Fig. 1D). Phosphorylation of HER2^{WT}, but not HER2^{L869R}, was blocked by the reversible HER2/EGFR TKI lapatinib, whereas neratinib inhibited phosphorylation of both WT and mutant receptors. Expression of HER2^{L869R} enhanced MCF10A cell proliferation in growth factor-depleted media (Fig. 1E) and colony formation in 3D Matrigel in the absence of EGF and insulin (Fig. 1F) compared to MCF10A/HER2^{WT} cells. Growth of MCF10A/HER2^{L869R} cells was inhibited by neratinib but not by lapatinib, whereas the HER2^{WT} cells were sensitive to both TKIs. With these supporting data, the patient was enrolled in a clinical trial with single agent neratinib (NCT01953926). Upon treatment, the patient exhibited an excellent clinical response, showing near disappearance of multiple skin metastases after 20 days (Fig. 1G), and a 77% reduction in marker lesions by RECIST criteria after 8 weeks.

Since the patient harbored a co-occurring *ERBB3*^{E928G} mutation, a known activating mutation in HER3 (15), we next asked whether HER2^{L869R} and HER3^{E928G} might cooperate to drive HER2 signaling. Mutations in *ERBB2* and *ERBB3* often co-occur in cancer. In the AACR Project GENIE dataset (>18,000 sequenced tumors), 8.3% of *ERBB2*-mutated cancers also harbor mutations in *ERBB3*, whereas only 2.3% of *ERBB2* WT cancers have *ERBB3* mutations (q value=1.3×10⁻¹⁰; www.cbioportal.org/genie). *ERBB2*^{L869R} and *ERBB3*^{E928G} were found to co-occur in another breast cancer case in the METABRIC data set (16). Structural modeling of the HER2^{L869R}/HER3^{E928G} double-mutant predicted that the HER3 mutation, located at the dimer interface, may enhance heterodimerization of the kinase domains through decreased bulk and electrostatic repulsion (Fig. S1A). Calculating the change in free energy of WT heterodimers compared to mutant heterodimers demonstrated a significant difference in the capacity of the latter to bind to one

another (Fig. S1B). Further, co-expression of the HER2^{L869R} and HER3^{E928G} intracellular domains (ICDs) resulted in enhanced transphosphorylation of HER3 and ERK as substrates compared to that induced by expression of either mutant alone (Fig. S1C). Phosphorylation of mutant HER2 and HER3, as well as the elevated downstream signaling induced by expression of both mutants, was blocked by treatment with neratinib (Fig. S1D). These data suggest that these co-occurring mutations in *ERBB2* and *ERBB3* enhance ERBB signaling output which, in turn, can be blocked by neratinib.

Acquired HER2^{T798I} mediates neratinib resistance

After 5 months on therapy, the patient developed a painful metastasis in the sternum. Addition of the estrogen receptor antagonist fulvestrant to neratinib induced a prompt symptomatic and clinical response. After 10 additional months on the combination, the patient progressed with new skin metastases. Targeted tissue-based NGS analysis of DNA from a new skin metastasis and plasma tumor, cell-free (cf) DNA (Guardant360™) revealed that *ERBB2*^{L869R} remained (44% allele frequency and 8.7% cfDNA, respectively; Supplementary Table S3). *ERBB3*^{E928G} remained in the post-treatment biopsy as well. *ERBB2*^{T798I} was found in plasma (1.3% cfDNA), but not in DNA from the synchronous skin metastasis. Additional single-gene deep sequencing of plasma *ERBB2* using two rounds of targeted capture (average >4,000 reads per sample) in an independent plasma sample from that used for the Guardant360 test failed to identify *ERBB2*^{T798I} in any of the plasma samples obtained at study enrollment or during the first 9 cycles of neratinib, but increased to 1.0% of reads at the time of clinical progression (Fig. 2A and Supplementary Table S4). In contrast, *ERBB2*^{L869R} was detected in 6.8% of reads in the pre-treatment sample, decreasing considerably during therapy, and rebounding up to 15.2% at progression. These data suggest that *ERBB2*^{T798I} was acquired during neratinib therapy.

HER2^{T798I} is homologous to EGFR^{T790M} and imatinib-resistant KIT^{T670I} in gastrointestinal stromal tumors (GIST) (Fig. 2B). EGFR^{T790M} drives resistance to first- and second-generation EGFR TKIs in NSCLC by two mechanisms: first, by mediating steric hindrance of ATP-competitive drugs, and second, by increasing the affinity of ATP resulting in enhanced phosphotransfer and kinase activity (17). To determine whether HER2^{T798I} functions in a similar manner, we constructed computational models of HER2^{WT} and HER2^{T798I} bound to neratinib. We found that the increased bulk of the isoleucine at position 798 would result in steric hindrance when neratinib binds (Fig. 2C). The closest approach between non-hydrogen atoms from residue T798 to neratinib is 4.1 Angstrom in HER2^{WT}, whereas this distance is reduced to 3.6 Angstrom in HER2^{T798I}, resulting in a reduced size of the binding pocket. Therefore, the isoleucine substitution at position 798 is expected to reduce neratinib binding.

Next, we asked whether the T798I mutation would block neratinib action. HEK293 cells transfected with HER2^{WT}, HER2^{L869R}, HER2^{T798I}, or HER2^{L869R/T798I} (both mutations *in cis*) were treated with increasing doses of neratinib for 4 h. Low doses of neratinib (20 nM) blocked pHER2, pAKT and pERK in cells expressing HER2^{WT} or HER2^{L869R}, but not in cells expressing HER2^{T798I} or HER2^{L869R/T798I} treated with up to 180 nM neratinib (Fig. 2D). To confirm these findings, we stably transduced MCF10A cells with WT and mutant

HER2. We noted that HER2^{T798I} and HER2^{T798I/L869R} were poorly expressed in HEK293 and MCF10A cells (Fig. 2D,E). Treatment with the proteasome inhibitor MG132 for 24 h restored expression of the T798I mutants (Fig. S2), suggesting that this mutation decreases protein stability. Cells expressing HER2^{L869R} or HER2^{L869R/T798I}, but not HER2^{T798I} alone, displayed enhanced pAKT, pERK and pS6 (Fig. 2E). Furthermore, while HER2^{L869R} and HER2^{L869R/T798I} induced EGF-independent MCF10A cell proliferation, HER2^{T798I} did not (Fig. 2F). Although untreated MCF10A/HER2^{L869R/T798I} cells did not proliferate as fast as cells expressing HER2^{L869R}, they were the only cells that grew in the presence of neratinib. A similar slow growth rate has been reported in EGFR TKI-resistant cell lines and patients' tumors harboring EGFR^{T790M} (18). MCF10A cells expressing both mutations displayed reduced sensitivity to neratinib (IC₅₀=154 nM) compared to cells expressing HER2^{L869R} (IC₅₀=23.9 nM; Fig. 2G). These results suggest that, like EGFR^{T790M} for gefitinib and erlotinib, HER2^{T798I} confers a growth advantage in the presence of neratinib.

The lack of transforming capacity of HER2^{T798I} alone suggests that it is not a driver oncogene, but an acquired alteration as a result of therapeutic pressure. Consistent with this speculation, HER2^{T798I} is exceedingly rare in tumors from patients not treated with HER2 TKIs (Supplementary Table S2). Out of all of the tumors sequenced in cBioPortal, COSMIC, Foundation Medicine, and Guardant Health databases (over 100,000 samples sequenced in all), HER2^{T798I} was only found in one colorectal cancer (Foundation Medicine) and in one endometrial cancer cell line (CCLE), strongly suggesting that in the patient reported herein, T798I was acquired due to selective pressure of neratinib treatment.

We next examined a panel of other irreversible EGFR/HER2 TKIs for their ability to block HER2^{L869R/T798I}. These included afatinib, a covalent EGFR/HER2 inhibitor, the EGFR inhibitor osimertinib (AZD9291), which exhibits selectivity against mutant EGFR (including T790M) but does not block WT HER2 (19), and AZ5104, an osimertinib metabolite that inhibits WT HER2 and EGFR (20). We performed computational modeling of HER2^{L869R/T798I} bound to neratinib, afatinib, osimertinib, and AZ5104 (Fig. 3A–D). These small molecules are expected to bind HER2 using the same mechanism and position by which they bind EGFR. By analogy with EGFR, the HER2 kinase is predicted to adopt distinct conformations when bound by each inhibitor. Afatinib and neratinib have covalent binding modes that project deeply into the substrate binding pocket of the HER2 kinase (Fig. 3A,B). The sterically larger side chain of HER2^{T798I} decreases the available space and decreases the polar character of the binding pocket. This is predicted to affect neratinib binding, which, by being the largest of these small molecules, extends the deepest into the pocket. While afatinib is predicted to make slight contact with T798I, it does not insert as far into the tunnel as neratinib does. Osimertinib and AZ5104 are predicted to bind much less deeply on the lip of the pocket (Fig. 3C,D). Based on these studies, HER2^{T798I} is predicted to disrupt neratinib binding, but is not expected to significantly affect the binding of afatinib, osimertinib, or AZ5104.

We next tested the ability of the panel of inhibitors to block mutant HER2 in stably transduced NR6 mouse fibroblasts, which lack endogenous EGFR (21), and MCF10A cells. In both cell types, neratinib more efficiently blocked pHER2 in cells expressing HER2^{WT} or HER2^{L869R} compared to cells expressing HER2^{L869R/T798I} (Fig. 3E, F). Treatment with

afatinib and AZ5104 blocked phosphorylation of HER2^{WT} as well as both HER2 mutants. In contrast, osimertinib failed to inhibit HER2^{WT}, HER2^{L869R} or HER2^{T798I}. Inhibition of pAKT, pERK, and pS6 with all small molecules mirrored that of pHER2 in MCF10A cells (Fig. 3F).

MCF10A/HER2^{L869R} and MCF10A/HER2^{L869R/T798I} were highly sensitive to afatinib and AZ5104 in growth factor-depleted media, whereas higher doses of osimertinib were required to block the growth of both cell types (Fig. 4A). Neratinib and AZ5104 showed similar IC₅₀ values in HER2^{L869R}-expressing cells, whereas neratinib was less effective against HER2^{L869R/T798I}-expressing cells. In 3D Matrigel, 100 nM of neratinib, afatinib, or AZ5104 completely blocked acini formation by MCF10A/HER2^{L869R} cells, whereas 100 nM of osimertinib only slightly suppressed acini growth (Fig. 4B). Both neratinib and osimertinib failed to suppress growth of MCF10A/HER2^{L869R/T798I} cells in 3D Matrigel, whereas this was completely blocked by afatinib and AZ5104, suggesting that the latter two inhibitors are able to overcome HER2^{T798I}-mediated drug resistance.

Recent reports have proposed the acquisition of HER2 mutations in patients with WT HER2 amplification treated with anti-HER2 therapies (22). In addition, neratinib has shown clinical activity and is being used in patients with WT HER2 amplification (23). Thus, we tested if a HER2 gatekeeper mutation would confer resistance to neratinib when present in a background of WT HER2 amplification. We used HER2-amplified BT474 cells stably expressing HER2^{T798M}, which we previously reported to be lapatinib-resistant (24). BT474^{GFP} control cells and BT474^{HER2-T798M} cells were treated with vehicle (DMSO), lapatinib, neratinib, afatinib, osimertinib or AZ5104. Lapatinib failed to suppress pHER2, pAKT, pERK and pS6 in HER2^{T798M}-expressing cells (Fig. 4C). Treatment with neratinib inhibited pHER2, pAKT and pS6 in BT474^{GFP} cells but not in BT474^{HER2-T798M} cells. Consistent with the findings in MCF10A cells, afatinib and AZ5104, but not osimertinib, blocked pAKT, pERK, and pS6 in both BT474^{GFP} and BT474^{HER2-T798M} cells. Since only ~3% of the *ERBB2* alleles in the BT474^{HER2-T798M} cells harbor the mutation (24), these data suggest that just a few HER2^{T798M} alleles can confer resistance to neratinib, but not afatinib, in cells with WT HER2 gene amplification.

Discussion

We report herein the identification of a HER2^{T798I} gatekeeper mutation in a patient with HER2-mutant, non-amplified breast cancer with acquired resistance to neratinib. Structural modeling showed that the T798I mutation results in a steric clash with neratinib, which would reduce drug binding. HER2^{T798I} directly promoted resistance to neratinib in lentivirally-transduced cell lines. In contrast to neratinib, afatinib and the metabolite of osimertinib, AZ5104, blocked HER2^{T798I}-induced signaling and cell growth.

While the initial neratinib-sensitizing HER2^{L869R} mutation induced constitutive phosphorylation of AKT, ERK, and S6, and displayed gain-of-function activity when expressed in breast epithelial cells (Fig. 1), we failed to observe increased phosphorylation of this mutant compared to WT HER2 (Figs. 1D; 2D,E). We speculate that the L869R mutation likely removes autoinhibitory interactions, thus placing the kinase in a better

position to interact with other ERBB receptors and adaptor proteins/downstream substrates (25,26). Notably, the HER2 mutant cancer also harbored a known activating HER3^{E928G} mutation (15). We speculate these co-mutations resulted in increased dependence on the ERBB pathway and contributed to the tumor's initial sensitivity to neratinib. Consistent with this speculation, preliminary results from the SUMMIT trial show that among 17 patients who exhibited clinical benefit from neratinib, 2 patients harbored *ERBB3* missense mutations, whereas none of the 25 patients who did not benefit harbored *ERBB3* alterations in their cancer (27).

Our findings parallel the identification of the EGFR^{T790M} gatekeeper mutation in NSCLC resistant to EGFR inhibitors. We note that for *EGFR*, 2 nucleotides would need to be mutated to change the threonine codon at position 790 to an isoleucine [ACG (Thr) > ATA, ATC, or ATT (Ile)], whereas only one nucleotide change is needed for the T790M mutation (ACG>ATG). The opposite is true for *ERBB2* [ACA (Thr) > ATA (Ile) vs ACA > ATG (Met)]. Thus, it is easier for the tumor to mutate *ERBB2* codon 798 to an isoleucine rather than a methionine.

EGFR^{T790M} is reported to promote resistance by simultaneously increasing ATP affinity and decreasing drug binding (28). While our data suggest that the HER2^{T798I} mutation could affect neratinib binding through steric interactions, it could similarly affect ATP binding and kinase activity. Although the change in distance (0.5 Angstrom) from residue 798 to neratinib could theoretically be accommodated by conformational changes, the structural evidence suggests that replacing a polar amino acid (Thr) with a hydrophobic residue (Ile) would *decrease* ATP affinity. The wild-type Thr side chain contains an -OH group that faces the ATP binding site. In the AMP-PNP-bound crystal structure of EGFR (2GS7.pdb), that -OH group is within 3.4 Angstrom of the N6 of AMP-PNP. Replacing the Thr with Ile would remove that favorable interaction and is expected to decrease ATP affinity. These structural assessments are consistent with our cell-based findings that T798I-expressing cells do not show increased HER2 phosphorylation, even when corrected for expression levels (Fig. 2D–E).

HER2^{T798I} and EGFR^{T790M} also differ in that the former is exceedingly rare in untreated tumors (Supplementary Table S2) whereas EGFR^{T790M} also occurs in germline DNA and can promote lung cancer formation (29), suggesting that EGFR^{T790M} itself is oncogenic. This is also consistent with the notion that HER2^{T798I} alone is not oncogenic, but requires another activating mutation in cis (e.g., L869R) to promote HER2 signaling and oncogenic growth (Fig. 2).

We previously reported that a HER2^{T798M} gatekeeper mutation increased HER2 autophosphorylation and association of HER3 with the p85 regulatory subunit of PI3K (24). In the current study, HER2^{T798I} alone did not appear to enhance HER2 signaling or HER2-induced proliferation more than WT HER2 (Fig. 2E,F). This discrepancy may be due to differences in experimental conditions (i.e., serum starvation), differences between the Met and Ile residues, or lower expression of the mutant receptor compared to WT, which we observed in multiple cell lines expressing T798I alone or in cis with L869R (Figs. 2E, 3E). We speculate that the decreased expression of the mutant may be due to decreased protein

stability (Supplementary Fig. S2). Despite this decreased expression, MCF10A cells expressing HER2^{T798I/L869R} displayed increased phosphorylation of HER2 signaling targets and EGF-independent proliferation compared to MCF10A/HER2^{WT} cells, as well as robust growth in the presence of neratinib (Figs. 2E–G, 4B), altogether suggesting that even low levels of HER2^{T798I} can promote neratinib resistance.

We are unable to determine whether *ERBB2*^{L869R} and *ERBB2*^{T798I} occur in cis in the patient's plasma, since these two mutations are 213 bp apart, longer than the length of cfDNA fragments shed from tumor cells. In NSCLC, *EGFR*^{T790M} is usually found on the same allele as the initial TKI-sensitizing EGFR mutation (30), suggesting that the two *ERBB2* mutations may also occur in cis. Additionally, the allele frequency of *ERBB2*^{T798I} in plasma tumor cell free DNA in the patient progressing on neratinib was lower than the frequency of *ERBB2*^{L869R} (Fig. 2A and Supplementary Table S3) consistent with HER2^{L869R} being the initial driver mutation, and HER2^{T798I} representing an acquired subclonal drug-resistant mutation. A similar relationship is typically seen with somatic *EGFR*^{T790M} in the plasma of patients progressing on EGFR inhibitors compared to the level of the original drug-sensitive EGFR mutation (31). We also note that HER2^{T798I} was not found in a new skin metastasis synchronous with the progression on neratinib, suggesting spatially heterogeneous mechanisms of drug resistance. This finding is consistent with other reports where plasma may serve as a repository of different acquired drug-resistant mutations found in some but not all metastatic sites, whereas a tissue biopsy of a single lesion may produce a less complete picture, as suggested by studies with drug-resistant NSCLC expressing *EGFR*^{T790M}. For example, a subset of patients with EGFR TKI-resistant NSCLC with *EGFR*^{T790M} detected in plasma but not in a tumor biopsy still responded to osimertinib (32).

PIK3CA^{M1043I}, an activating mutation in the p110 α catalytic subunit of PI3K (33), was found at 0.1% frequency in the same plasma sample where HER2^{T798I} was first detected (Supplementary Table S3). *PIK3CA* mutations are associated with resistance to anti-HER2 therapy in HER2-overexpressing breast cancers (34). Whether *PIK3CA*^{M1043I} contributes to a multifactorial resistance to neratinib is also possible but beyond the scope of this report. While afatinib and neratinib are both irreversible covalent EGFR/HER2 TKIs, we found that afatinib, but not neratinib, was able to block HER2^{L869R/T798I} activity. We speculate that because neratinib is larger than afatinib, the former is more likely to be affected by a steric clash with the bulkier isoleucine residue in HER2^{T798I} (Fig. 3A,B). Treatment with low doses of afatinib (10 nM), easily achievable in patients (35), completely blocked growth of MCF10A/HER2^{L869R/T798I} cells, while treatment with neratinib at clinically achievable concentrations (36) failed to do so (Fig. 4A,B). We also observed moderate activity of the osimertinib metabolite AZ5104 (Fig. 4). However, this drug is not being developed independently of osimertinib, and only ~10% of osimertinib is metabolized into AZ5104 in humans (20).

Immediately following progression on neratinib, the patient was treated with capecitabine chemotherapy. The patient responded well and remains in a partial response ~one year later. We repeated next gen sequencing of her plasma tumor DNA after ~6 months on capecitabine; *ERBB2*^{L869R} cfDNA dropped to 0.4%, while *ERBB2*^{T798I} and *CCND1*

amplification were no longer detectable, consistent with the decrease in tumor burden and the patient's clinical response. If the patient progresses on capecitabine and the *ERBB2* mutations are once again detectable, there will be strong consideration for treatment with afatinib at this time. As more patients with HER2-mutant cancers are treated with HER2 TKIs such as neratinib, we expect that acquired HER2^{T798I} may be observed more frequently. We propose afatinib is active against HER2^{T798I} and is an alternative worthy of clinical investigation in cancers harboring the HER2 gatekeeper mutation. Finally, this report supports the development of HER2^{T798I}-selective inhibitors that would spare the toxicity associated with therapeutic inhibition of WT ERBB receptors.

Methods

ERBB2 Single-Gene Targeted Capture

Extraction of cell free DNA from plasma was performed using a fully automated QIAGEN platform, QIAAsymphony SP, and QIAAsymphony DSP Virus/Pathogen Midi Kit following centrifugation. Sequence libraries were prepared according to the KAPA Hyper protocol (Kapa Biosystems) with the ligation of Illumina sequence adaptors followed by PCR amplification and clean-up. Barcoded libraries were hybridized with DNA probes targeting all coding exons of *ERBB2* (Integrated DNA Technologies) in two successive captures, using a protocol modified from the NimbleGen SeqCap Target Enrichment system. The first capture was incubated at 55°C for 16 h followed by post-capture washes and 16 cycles of PCR amplification. The second capture was incubated at 65°C for 4 h followed by post-capture washes and 3–5 cycles of PCR amplification. Captured libraries were sequenced on an Illumina HiSeq as paired-end 100 bp reads.

Computational modeling

Structural modeling of inhibitor-bound HER2^{WT}, HER2^{L869R}/HER3^{E928G} and HER2^{L869R/T798I} was performed using Rosetta. Detailed procedures are available in Supplementary Methods.

Cell lines and inhibitors

MCF10A breast epithelial cells (ATCC® CRL-10317TM; purchased in 2012) and HEK293 human embryonic kidney cells (ATCC® CRL-1573TM; purchased in 2006) were from ATCC. Cell lines were authenticated by ATCC prior to purchase by the short tandem repeat (STR) method. 293FT cells were purchased from Invitrogen (Cat. No. R70007). NR6 cells have been previously described (21), as have BT474^{GFP} and BT474^{HER2^{T798M}} (24). *ERBB2*^{T798M} was verified by sequencing cDNA using primers for *ERBB2*. Other than routinely checking cell morphology for consistency with published images, no other authentication was performed.

293FT, HEK293, and NR6 cells were maintained in DMEM supplemented with 10% FBS and 1X Antibiotic-Antimycotic (Gibco). BT474 cells were maintained in IMEM supplemented with 10% FBS, 1X Antibiotic-Antimycotic, and 100 µg/ml G418. MCF10A cells were maintained in MCF10A complete media (DMEM/F12 supplemented with 5% horse serum, 20 ng/ml EGF, 10 µg/ml insulin, 0.5 µg/ml hydrocortisone, 0.1 µg/ml cholera

toxin, and 1X antibiotic/antimycotic). For experiments under growth factor-depleted conditions, MCF10A cells were grown in DMEM/F12 supplemented with 1% charcoal/dextran-stripped serum (CSS), 10 µg/ml insulin, 0.5 µg/ml hydrocortisone, 0.1 µg/ml cholera toxin, and 1X Antibiotic-Antimycotic. Cell lines were routinely evaluated for *mycoplasma* contamination. All experiments were completed less than 2 months after thawing early-passage cells.

The following inhibitors were used: MG132 (Selleck Chemicals), lapatinib (LC Laboratories), neratinib (PUMA Biotechnology), afatinib (Selleck Chemicals), and osimertinib and AZ5104 (AstraZeneca Pharmaceuticals).

Immunoblot analysis

Cells were washed with PBS and lysed on ice in RIPA lysis buffer plus protease and phosphatase inhibitors. Protein concentration was measured using the BCA protein assay reagent (Pierce). Lysates were subjected to SDS-PAGE and transferred to nitrocellulose membranes (Bio-Rad). Immunoreactive bands were detected by enhanced chemiluminescence following incubation with horseradish peroxidase-conjugated secondary antibodies (Promega). Detailed information on antibodies is available in Supplementary Methods. Immunoblot bands were quantified from inverted images using ImageJ software.

Cell growth assays

MCF10A cells were seeded in black clear-bottom 96-well plates (Greiner Bio-One) at a density of 1,000 cells per well in growth factor-depleted media. The next day, media was replaced with 100 µl media containing increasing amounts of inhibitor (0.17 nM–10 µM in 3-fold dilutions). After 5–6 days, nuclei were stained with 10 µg/ml Hoechst 33342 (Thermo Fisher Scientific) at 37°C for 20 min. Fluorescent nuclei were counted using the ImageXpress Micro XL automated microscope imager (Molecular Devices).

For three-dimensional (3D) growth assays, cells were seeded on growth factor-reduced Matrigel (BD Biosciences) in 48-well plates following published protocols (37). Inhibitors were added to the medium at the time of cell seeding. Fresh media and inhibitors were replenished every 3 days. Following 9–14 days, colonies were stained with 5 mg/ml MTT for 20 min. Plates were scanned and colonies measuring 100 µm were counted using GelCount software (Oxford Optronix). Colonies were photographed using an Olympus DP10 camera mounted in an inverted microscope.

Patient studies

Informed consent was obtained from the patient described in this study. The clinical trial (NCT01953926) was conducted in accordance with the Declaration of Helsinki and approved by an institutional review board.

Statistical analysis

All experiments were performed using at least three technical replicates and at least two independent times. P values were generated by ANOVA followed by Tukey's multiple

comparisons test unless otherwise indicated. Data are presented as mean \pm SD. IC₅₀ values were generated through GraphPad Prism (version 6.0).

Detailed descriptions of NGS, multiple sequence alignment, determination of mutation frequencies, transient transfections, and generation of stable cell lines are available in Supplementary Methods.

Supplementary Material

Refer to Web version on PubMed Central for supplementary material.

Acknowledgments

Financial Support: This work was supported by NIH/NCI K12 Award CA090625 (ABH); NCI R01 grant CA080195 (CLA); ACS Clinical Research Professorship Award CRP-07-234-06-COUN (CLA); a research grant from Puma Biotechnology; NIH Breast Cancer Specialized Program of Research Excellence (SPORE) grant P50 CA098131; and Vanderbilt-Ingram Cancer Center Support Grant P30 CA68485.

We would like to acknowledge the American Association for Cancer Research and its support in the development of the AACR Project GENIE registry, as well as members of the consortium for their commitment to data sharing. Interpretations are the responsibility of study authors. In addition, we offer our sincere gratitude to the patient for her contribution to this study.

References

1. Koboldt DC, Fulton RS, McLellan MD, Schmidt H, Kalicki-Veizer J, McMichael JF, et al. Comprehensive molecular portraits of human breast tumours. *Nature*. 2012; 490(7418):61–70. DOI: 10.1038/nature11412 [PubMed: 23000897]
2. Ross JS, Gay LM, Wang K, Ali SM, Chumsri S, Elvin JA, et al. Nonamplification ERBB2 genomic alterations in 5605 cases of recurrent and metastatic breast cancer: An emerging opportunity for anti-HER2 targeted therapies. *Cancer*. 2016; 122(17):2654–62. DOI: 10.1002/cncr.30102 [PubMed: 27284958]
3. Chmielecki J, Ross JS, Wang K, Frampton GM, Palmer GA, Ali SM, et al. Oncogenic alterations in ERBB2/HER2 represent potential therapeutic targets across tumors from diverse anatomic sites of origin. *Oncologist*. 2015; 20(1):7–12. DOI: 10.1634/theoncologist.2014-0234 [PubMed: 25480824]
4. Desmedt C, Zoppoli G, Gundem G, Pruneri G, Larsimont D, Fornili M, et al. Genomic Characterization of Primary Invasive Lobular Breast Cancer. *J Clin Oncol*. 2016; 34(16):1872–81. DOI: 10.1200/JCO.2015.64.0334 [PubMed: 26926684]
5. Bose R, Kavuri SM, Searleman AC, Shen W, Shen D, Koboldt DC, et al. Activating HER2 mutations in HER2 gene amplification negative breast cancer. *Cancer discovery*. 2013; 3(2):224–37. DOI: 10.1158/2159-8290.CD-12-0349 [PubMed: 23220880]
6. Wang SE, Narasanna A, Perez-Torres M, Xiang B, Wu FY, Yang S, et al. HER2 kinase domain mutation results in constitutive phosphorylation and activation of HER2 and EGFR and resistance to EGFR tyrosine kinase inhibitors. *Cancer Cell*. 2006; 10(1):25–38. S1535-6108(06)00179-6 [pii]. DOI: 10.1016/j.ccr.2006.05.023 [PubMed: 16843263]
7. Minami Y, Shimamura T, Shah K, LaFramboise T, Glatt KA, Liniker E, et al. The major lung cancer-derived mutants of ERBB2 are oncogenic and are associated with sensitivity to the irreversible EGFR/ERBB2 inhibitor HKI-272. *Oncogene*. 2007; 26(34):5023–7. DOI: 10.1038/sj.onc.1210292 [PubMed: 17311002]
8. Greulich H, Kaplan B, Mertins P, Chen TH, Tanaka KE, Yun CH, et al. Functional analysis of receptor tyrosine kinase mutations in lung cancer identifies oncogenic extracellular domain mutations of ERBB2. *Proc Natl Acad Sci U S A*. 2012; 109(36):14476–81. DOI: 10.1073/pnas.1203201109 [PubMed: 22908275]

9. Kavuri SM, Jain N, Galimi F, Cottino F, Leto SM, Migliardi G, et al. HER2 activating mutations are targets for colorectal cancer treatment. *Cancer discovery*. 2015; 5(8):832–41. DOI: 10.1158/2159-8290.CD-14-1211 [PubMed: 26243863]
10. Frampton GM, Fichtenholtz A, Otto GA, Wang K, Downing SR, He J, et al. Development and validation of a clinical cancer genomic profiling test based on massively parallel DNA sequencing. *Nature biotechnology*. 2013; 31(11):1023–31. DOI: 10.1038/nbt.2696
11. Wong DJ, Ribas A. Targeted Therapy for Melanoma. *Cancer Treat Res*. 2016; 167:251–62. DOI: 10.1007/978-3-319-22539-5_10 [PubMed: 26601866]
12. Kobayashi Y, Mitsudomi T. Not all epidermal growth factor receptor mutations in lung cancer are created equal: Perspectives for individualized treatment strategy. *Cancer Sci*. 2016; 107(9):1179–86. DOI: 10.1111/cas.12996 [PubMed: 27323238]
13. Leaver-Fay A, Tyka M, Lewis SM, Lange OF, Thompson J, Jacak R, et al. ROSETTA3: an object-oriented software suite for the simulation and design of macromolecules. *Methods Enzymol*. 2011; 487:545–74. DOI: 10.1016/B978-0-12-381270-4.00019-6 [PubMed: 21187238]
14. Yun CH, Boggon TJ, Li Y, Woo MS, Greulich H, Meyerson M, et al. Structures of lung cancer-derived EGFR mutants and inhibitor complexes: mechanism of activation and insights into differential inhibitor sensitivity. *Cancer Cell*. 2007; 11(3):217–27. S1535-6108(07)00028-1 [pii]. DOI: 10.1016/j.ccr.2006.12.017 [PubMed: 17349580]
15. Jaiswal BS, Kljavin NM, Stawiski EW, Chan E, Parikh C, Durinck S, et al. Oncogenic ERBB3 mutations in human cancers. *Cancer Cell*. 2013; 23(5):603–17. DOI: 10.1016/j.ccr.2013.04.012 [PubMed: 23680147]
16. Curtis C, Shah SP, Chin SF, Turashvili G, Rueda OM, Dunning MJ, et al. The genomic and transcriptomic architecture of 2,000 breast tumours reveals novel subgroups. *Nature*. 2012; 486(7403):346–52. DOI: 10.1038/nature10983 [PubMed: 22522925]
17. Eck MJ, Yun CH. Structural and mechanistic underpinnings of the differential drug sensitivity of EGFR mutations in non-small cell lung cancer. *Biochim Biophys Acta*. 2010; 1804(3):559–66. DOI: 10.1016/j.bbapap.2009.12.010 [PubMed: 20026433]
18. Chmielecki J, Foo J, Oxnard GR, Hutchinson K, Ohashi K, Somwar R, et al. Optimization of dosing for EGFR-mutant non-small cell lung cancer with evolutionary cancer modeling. *Sci Transl Med*. 2011; 3(90):90ra59.doi: 10.1126/scitranslmed.3002356
19. Berruti A, Brizzi MP, Generali D, Ardine M, Dogliotti L, Bruzzi P, et al. Presurgical systemic treatment of nonmetastatic breast cancer: facts and open questions. *Oncologist*. 2008; 13(11):1137–48. theoncologist.2008-0162 [pii]. DOI: 10.1634/theoncologist.2008-0162 [PubMed: 18997125]
20. Cross DA, Ashton SE, Ghiorghiu S, Eberlein C, Nebhan CA, Spitzler PJ, et al. AZD9291, an irreversible EGFR TKI, overcomes T790M-mediated resistance to EGFR inhibitors in lung cancer. *Cancer discovery*. 2014; 4(9):1046–61. DOI: 10.1158/2159-8290.CD-14-0337 [PubMed: 24893891]
21. Pruss RM, Herschman HR. Variants of 3T3 cells lacking mitogenic response to epidermal growth factor. *Proc Natl Acad Sci U S A*. 1977; 74(9):3918–21. [PubMed: 302945]
22. Trowe T, Boukouvala S, Calkins K, Cutler RE Jr, Fong R, Funke R, et al. EXEL-7647 inhibits mutant forms of ErbB2 associated with lapatinib resistance and neoplastic transformation. *Clin Cancer Res*. 2008; 14(8):2465–75. 14/8/2465 [pii]. DOI: 10.1158/1078-0432.CCR-07-4367 [PubMed: 18413839]
23. Chan A, Delaloge S, Holmes FA, Moy B, Iwata H, Harvey VJ, et al. Neratinib after trastuzumab-based adjuvant therapy in patients with HER2-positive breast cancer (ExteNET): a multicentre, randomised, double-blind, placebo-controlled, phase 3 trial. *Lancet Oncol*. 2016; 17(3):367–77. DOI: 10.1016/S1470-2045(15)00551-3 [PubMed: 26874901]
24. Rexer BN, Ghosh R, Narasanna A, Estrada MV, Chakrabarty A, Song Y, et al. Human breast cancer cells harboring a gatekeeper T798M mutation in HER2 overexpress EGFR ligands and are sensitive to dual inhibition of EGFR and HER2. *Clin Cancer Res*. 2013; 19(19):5390–401. DOI: 10.1158/1078-0432.CCR-13-1038 [PubMed: 23948973]

25. Zhang X, Gureasko J, Shen K, Cole PA, Kuriyan J. An allosteric mechanism for activation of the kinase domain of epidermal growth factor receptor. *Cell*. 2006; 125(6):1137–49. S0092-8674(06)00584-8 [pii]. DOI: 10.1016/j.cell.2006.05.013 [PubMed: 16777603]
26. Red Brewer M, Yun CH, Lai D, Lemmon MA, Eck MJ, Pao W. Mechanism for activation of mutated epidermal growth factor receptors in lung cancer. *Proc Natl Acad Sci U S A*. 2013; 110(38):E3595–604. DOI: 10.1073/pnas.1220050110 [PubMed: 24019492]
27. Hyman, DM., Piha-Paul, SA., Saura, C., Arteaga, C., Mayer, I., Shapiro, GI., et al. Neratinib + fulvestrant in ERBB2-mutant, HER2 non-amplified, estrogen receptor-positive, metastatic breast cancer: preliminary analysis from the phase II SUMMIT trial. Thirty-Ninth Annual CTRC-AACR San Antonio Breast Cancer Symposium; San Antonio, TX, USA. December 6–10, 2016;
28. Yun CH, Mengwasser KE, Toms AV, Woo MS, Greulich H, Wong KK, et al. The T790M mutation in EGFR kinase causes drug resistance by increasing the affinity for ATP. *Proc Natl Acad Sci U S A*. 2008; 105(6):2070–5. DOI: 10.1073/pnas.0709662105 [PubMed: 18227510]
29. Bell DW, Gore I, Okimoto RA, Godin-Heymann N, Sordella R, Mulloy R, et al. Inherited susceptibility to lung cancer may be associated with the T790M drug resistance mutation in EGFR. *Nat Genet*. 2005; 37(12):1315–6. ng1671 [pii]. DOI: 10.1038/ng1671 [PubMed: 16258541]
30. Pao W, Miller VA, Politi KA, Riely GJ, Somwar R, Zakowski MF, et al. Acquired resistance of lung adenocarcinomas to gefitinib or erlotinib is associated with a second mutation in the EGFR kinase domain. *PLoS Med*. 2005; 2(3):e73.doi: 10.1371/journal.pmed.0020073 [PubMed: 15737014]
31. Zheng D, Ye X, Zhang MZ, Sun Y, Wang JY, Ni J, et al. Plasma EGFR T790M ctDNA status is associated with clinical outcome in advanced NSCLC patients with acquired EGFR-TKI resistance. *Scientific reports*. 2016; 6:20913.doi: 10.1038/srep20913 [PubMed: 26867973]
32. Oxnard GR, Thress KS, Alden RS, Lawrance R, Paweletz CP, Cantarini M, et al. Association Between Plasma Genotyping and Outcomes of Treatment With Osimertinib (AZD9291) in Advanced Non-Small-Cell Lung Cancer. *J Clin Oncol*. 2016; 34(28):3375–82. DOI: 10.1200/JCO.2016.66.7162 [PubMed: 27354477]
33. Gymnopoulos M, Elsliger MA, Vogt PK. Rare cancer-specific mutations in PIK3CA show gain of function. *Proc Natl Acad Sci U S A*. 2007; 104(13):5569–74. DOI: 10.1073/pnas.0701005104 [PubMed: 17376864]
34. Arteaga CL, Engelman JA. ERBB receptors: from oncogene discovery to basic science to mechanism-based cancer therapeutics. *Cancer Cell*. 2014; 25(3):282–303. DOI: 10.1016/j.ccr.2014.02.025 [PubMed: 24651011]
35. Wind S, Schmid M, Erhardt J, Goeldner RG, Stopfer P. Pharmacokinetics of afatinib, a selective irreversible ErbB family blocker, in patients with advanced solid tumours. *Clinical pharmacokinetics*. 2013; 52(12):1101–9. DOI: 10.1007/s40262-013-0091-4 [PubMed: 23813493]
36. Wong KK, Fracasso PM, Bukowski RM, Lynch TJ, Munster PN, Shapiro GI, et al. A phase I study with neratinib (HKI-272), an irreversible pan ErbB receptor tyrosine kinase inhibitor, in patients with solid tumors. *Clin Cancer Res*. 2009; 15(7):2552–8. DOI: 10.1158/1078-0432.CCR-08-1978 [PubMed: 19318484]
37. Debnath J, Muthuswamy SK, Brugge JS. Morphogenesis and oncogenesis of MCF-10A mammary epithelial acini grown in three-dimensional basement membrane cultures. *Methods*. 2003; 30(3): 256–68. [PubMed: 12798140]

Statement of Significance

We found an acquired HER2 gatekeeper mutation in a patient with HER2-mutant breast cancer upon clinical progression on neratinib. We speculate that HER2^{T798I} may arise as a secondary mutation following response to effective HER2 TKIs in other cancers with HER2 activating mutations. This resistance may be overcome by other irreversible HER2 TKIs such as afatinib.

Author Manuscript

Author Manuscript

Author Manuscript

Author Manuscript

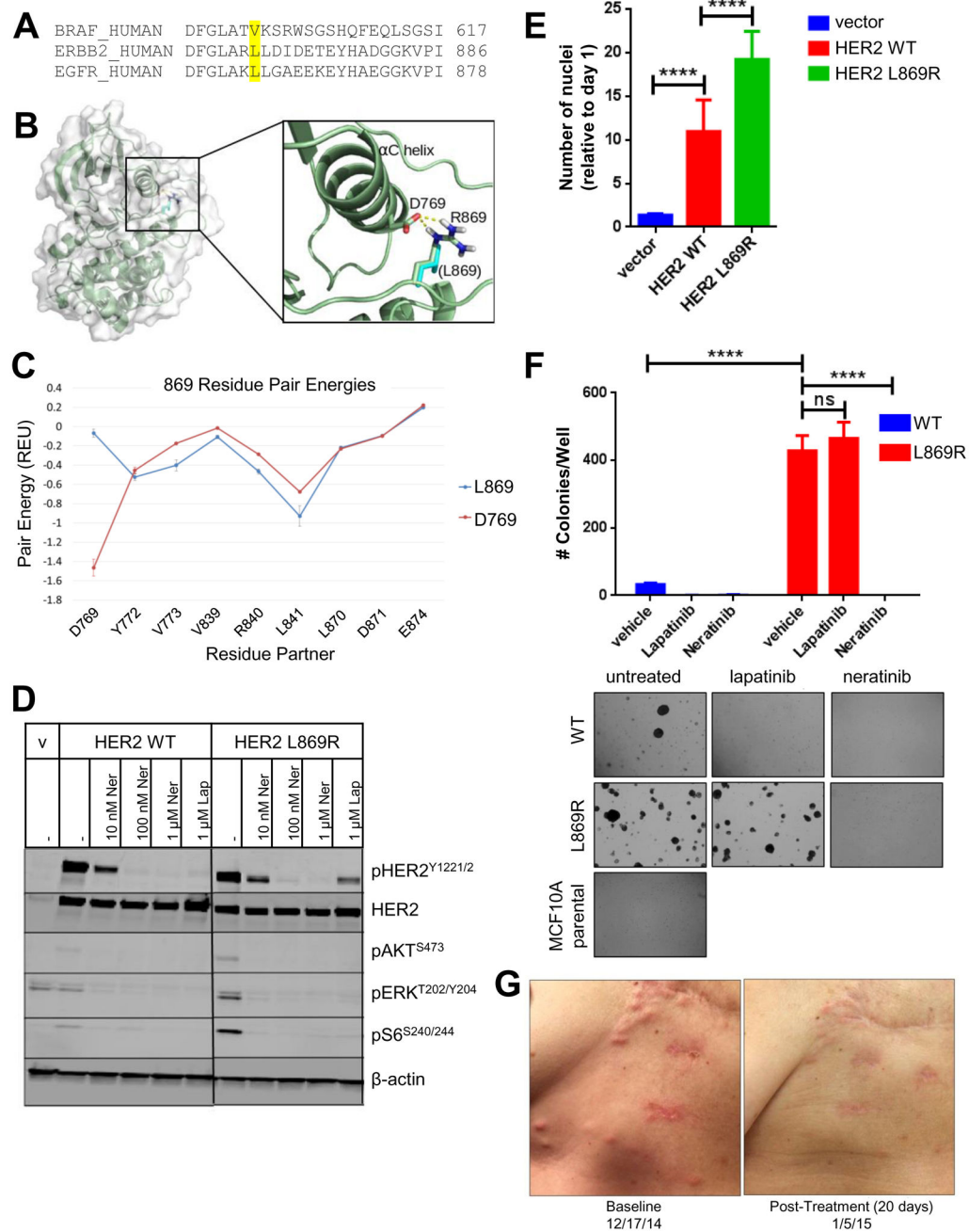


Fig. 1. HER2^{L869R} exhibits a gain-of-function phenotype that is blocked by neratinib
 (A) The amino acid sequences of human BRAF, ERBB2, and EGFR were aligned using Clustal Omega. BRAF V600, ERBB2 L869, and EGFR L861 residues are highlighted in yellow. (B) The structure of HER2^{L869R} was modeled. The mutation from Leucine (cyan) to Arginine (highlighted in blue) permits favorable charge interaction (dashed yellow lines) with Asp769. (C) Residue pair energies involving residue 869 reveal the addition of a strong attractive (negative) interaction at Asp769 in the HER2^{L869R} model. (D) MCF10A cells stably expressing HER2^{WT} or HER2^{L869R} were treated with vehicle (DMSO), 0.01–1.0 μM neratinib, or 1 μM lapatinib for 4 h in serum-free media. Cell lysates were probed with the

indicated antibodies. Scans are all from the same gel/film; the vertical black line indicates an irrelevant lane that was removed from the figure for clarity. (E) Stably transduced MCF10A cells were seeded in 96-well plates in MCF10A starvation media (1% charcoal-stripped serum, no EGF). After 7 days, nuclei were stained with Hoechst and scored using the ImageXpress system. Data points represent the average \pm standard deviation (SD) of 4 replicate wells (****, $p < 0.0001$, ANOVA followed by Tukey's multiple comparisons test). (F) Stably transduced MCF10A cells were plated in 3D Matrigel in presence of the indicated drugs (100 nM). Colonies were grown in media containing 5% charcoal-stripped serum without EGF and insulin. After ~2 weeks, colonies were stained with MTT and counted using the Gelcount system. Data represent the average \pm SD of 3 replicates. Representative fields (10X objective) of wells are shown below (**** $p < 0.0001$, ANOVA followed by Tukey's multiple comparisons test). (G) Chest wall skin metastases of patient with invasive lobular breast cancer harboring HER2^{L869R} at baseline and 20 days after starting treatment with neratinib.

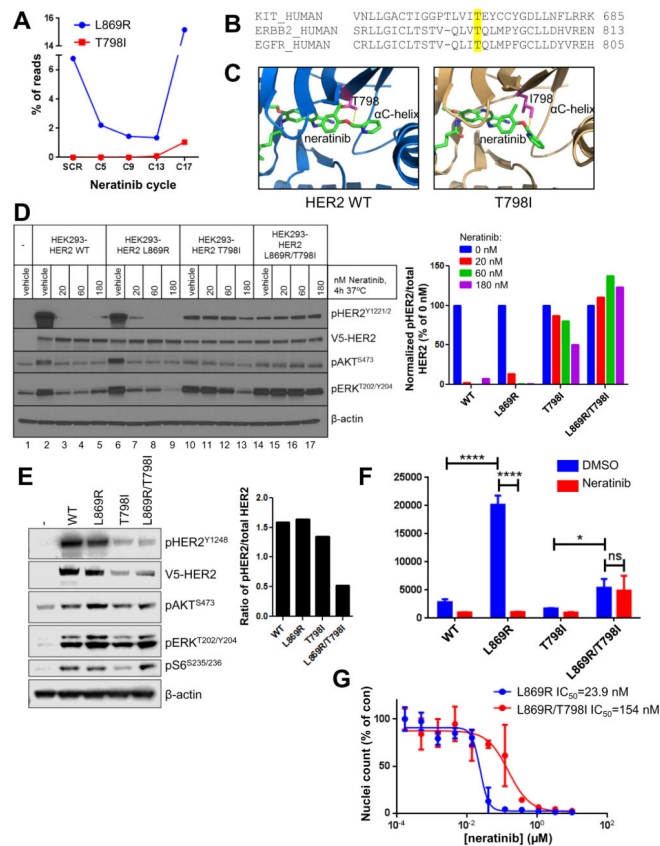


Fig. 2. HER2^{T798I} induces acquired resistance to neratinib

(A) The patient's plasma was drawn at the time of clinical trial screening (SCR) and the indicated cycles of neratinib therapy (1 cycle = 28 days). Plasma cfDNA was subjected to *ERBB2* targeted capture and sequenced. (B) The amino acid sequences of human KIT, ERBB2, and EGFR were aligned using Clustal Omega. KIT T670, ERBB2 T798, and EGFR T790 gatekeeper residues are highlighted in yellow. (C) The structure of HER2^{WT} and a model of HER2^{T798I} are shown with neratinib bound to the kinase pocket. The threonine (WT) or isoleucine (mutant) residue at position 798 is shown in pink. (D) HEK293 cells were transiently transfected with V5-tagged HER2^{WT}, HER2^{L869R}, HER2^{T798I} or HER2^{L869R/T798I} and treated with the indicated concentrations of neratinib for 4 h in serum-free media. Cell lysates were subjected to immunoblot analyses with the indicated antibodies. The bar graph represents quantification of immunoblot bands using ImageJ software. (E) MCF10A cells stably expressing V5- tagged HER2^{WT}, HER2^{L869R}, HER2^{T798I} or HER2^{L869R/T798I} were cultured in MCF10A growth factor-depleted media. Cell lysates were subjected to immunoblot analyses with the indicated antibodies. The bar graph represents quantification of immunoblot bands using ImageJ software. (F) MCF10A cells from (E) were treated ± 123 nM neratinib in growth factor-depleted media for 6 days. Nuclei were stained with Hoechst and scored using the ImageXpress system. Data represent the average ± SD of 4 replicate wells (*p<0.05, ****p<0.0001, ANOVA followed by Tukey's multiple comparisons test). (G) MCF10A cells stably expressing HER2^{L869R} (blue) or HER2^{L869R/T798I} (red) were treated with increasing concentrations of neratinib for 6 days.

Nuclei were stained with Hoechst and scored using the ImageXpress system. Data represent the average \pm SD of 4 replicate wells. IC₅₀ values were calculated using GraphPad Prism.

Author Manuscript

Author Manuscript

Author Manuscript

Author Manuscript

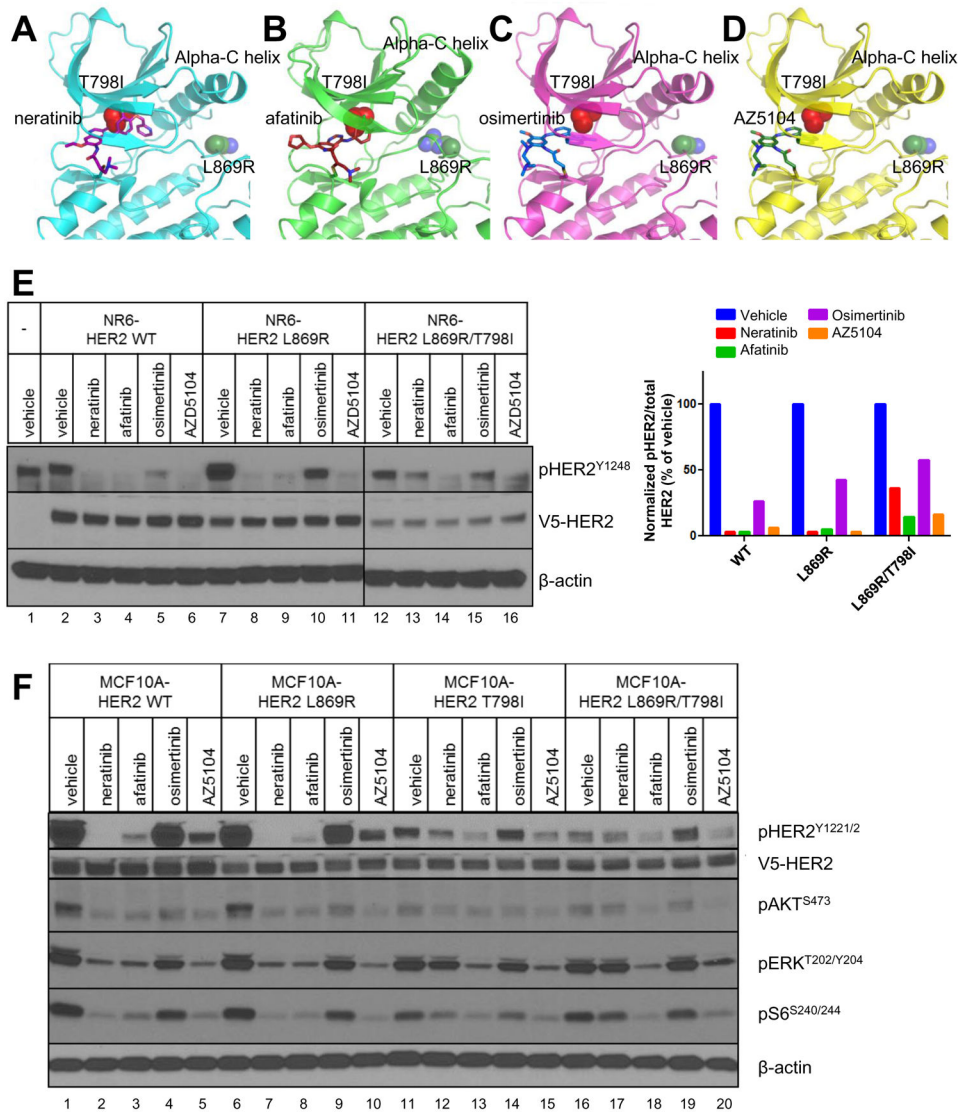


Fig. 3. Afatinib and AZ5104 block HER2^{L869R/T798I} signaling

(A–D) Computational modeling of the HER2 kinase domain in complex with (A) neratinib, (B) afatinib, (C) osimertinib, and (D) AZ5104 was performed. The N-terminal lobe and part of the C-terminal lobe of the tyrosine kinase domain (TKD) is shown in ribbon style. Each inhibitor is represented as sticks bound in the substrate-binding pocket. The T798I mutation is shown as red spheres deep in the pocket. The L869R mutation is shown as blue and green spheres on the far side of the alpha-C helix. (E) NR6 cells stably expressing V5-tagged HER2^{WT}, HER2^{L869R}, HER2^{T798I} or HER2^{L869R/T798I} (LR/TI) were treated with the indicated drugs at 100 nM for 4 h in serum-free media. Cell lysates were subjected to immunoblot analyses with the indicated antibodies. Scans are all from the same gel/film; the vertical black line indicates an irrelevant lane that was removed from the figure for clarity. The bar graph represents quantification of immunoblot bands using ImageJ software. (F) Stably transduced MCF10A cells were treated with the indicated drugs at 100 nM for 4 h in

EGF- and serum-free media. Cell lysates were subjected to immunoblot analyses with the indicated antibodies as described in Methods.

Author Manuscript

Author Manuscript

Author Manuscript

Author Manuscript

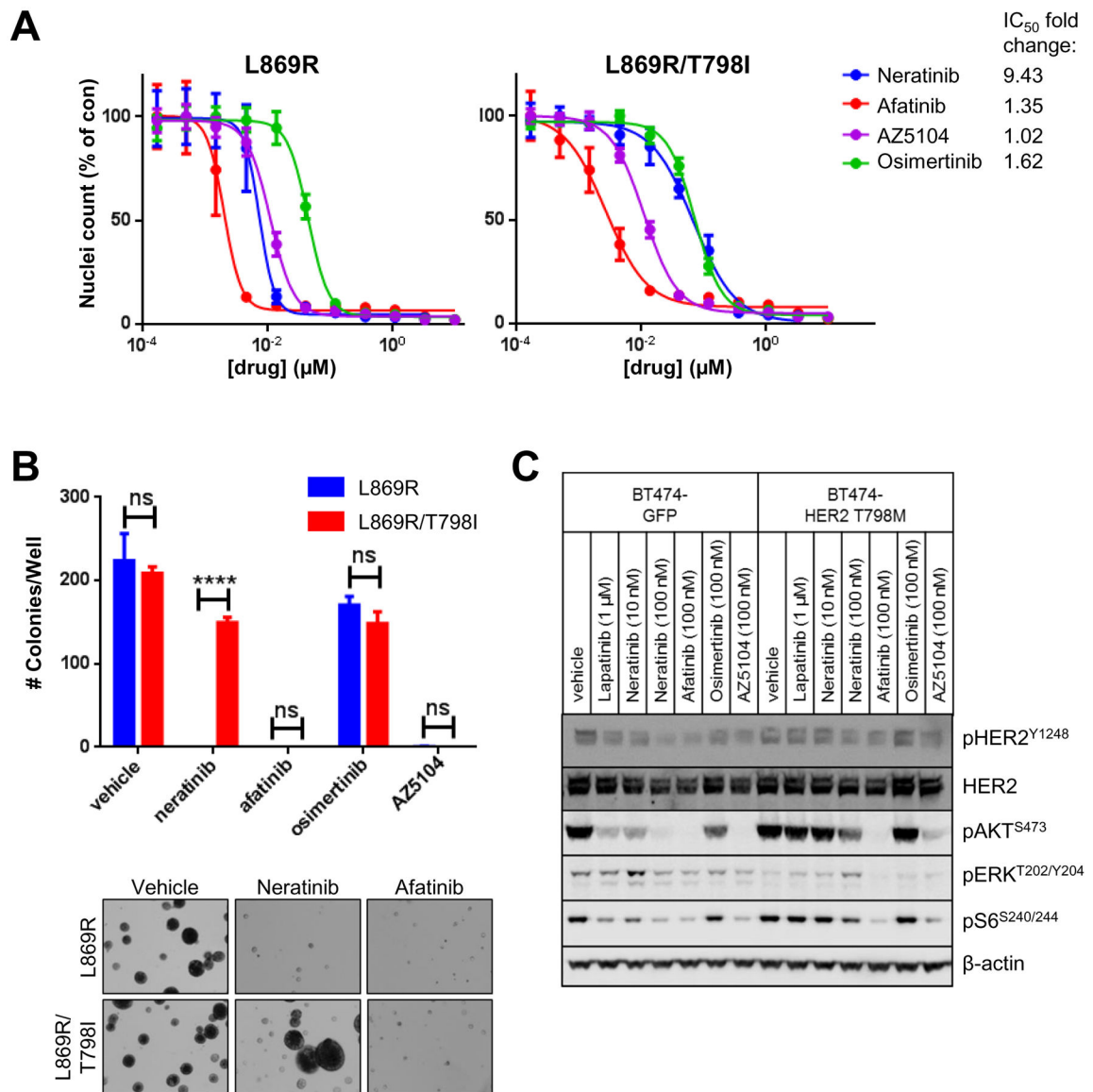


Fig. 4. Afatinib and AZ5104 block HER2^{L869R/T798I}-induced growth

(A) MCF10A cells stably expressing HER2^{L869R} and HER2^{L869R/T798I} were treated with increasing concentrations of neratinib, afatinib, osimertinib, or AZ5104. After 5 days, nuclei were stained with Hoechst and scored using the ImageXpress system. Data represent the average \pm SD of 4 replicate wells. The fold change in IC₅₀ values of MCF10A L869R/T798I cells relative to L869R cells is shown. (B) Stably transduced MCF10A cells were plated in 3D Matrigel in presence of the indicated drugs (100 nM). After 9 days, colonies were stained with MTT and counted using the Gelcount system. Data represent the average \pm SD of 3 replicates. Representative fields (10X objective) of wells treated with vehicle (DMSO), 100 nM neratinib, and 100 nM afatinib are shown (**** $p < 0.0001$, ANOVA followed by Tukey's multiple comparisons test). (C) BT474^{GFP} (control) and BT474^{HER2-T798M} were

treated with the indicated drugs for 4 h in serum-free media. Cells lysates were tested in immunoblot analyses using the indicated antibodies.

Author Manuscript

Author Manuscript

Author Manuscript

Author Manuscript